Article

Discovery Medicine 2026; 38(206): 866–876
https://doi.org/10.24976/Discov.Med.202638206.71

Wogonin Alleviates Insulin-Resistant PCOS by Targeting FN1 to Activate the PI3K/AKT Pathway

Li Yang[1], Fei Zhou[1], Da Li[1], Minghe Zhang[1], Wei Shen[1,*]

[1]Department of Endocrinology, The First People's Hospital of Xiaoshan District, Xiaoshan Affiliated Hospital of Wenzhou Medical University, 311201 Hangzhou, Zhejiang, China
*Correspondence: 18969957376@163.com (Wei Shen)
Submitted: 8 December 2025 Revised: 21 January 2026 Accepted: 4 February 2026 Published: 20 March 2026

Background: Insulin-resistant polycystic ovary syndrome (IR-PCOS) is a refractory endocrine disorder with limited therapeutic options. Wogonin, a natural flavonoid compound, has shown potential therapeutic efficacy; however, its underlying mechanism remains unclear. This study aimed to explore the therapeutic effects of wogonin on IR-PCOS and the mechanistic involvement of fibronectin 1 (FN1) and phosphatidylinositol 3-kinase (PI3K)/Protein kinase B (AKT) signaling pathway.
Methods: The interaction between wogonin and its potential target was predicted using molecular docking. An IR-PCOS mouse model was treated with wogonin alone or in combination with tail-vein injection of shFN1 or short hairpin negative control (shNC) lentiviral particles. Metabolic parameters, sex hormones, ovarian morphology, and key pathway proteins were assessed using glucose/insulin tolerance tests, enzyme-linked immunosorbent assays (ELISA), histopathology, and Western blotting.
Results: Molecular docking demonstrated a stable binding between wogonin and FN1. In IR-PCOS mice, wogonin significantly reduced body weight, restored serum sex hormone imbalances—characterized by decreased testosterone, estradiol, luteinizing hormone (LH), and the LH/follicle-stimulating hormone (FSH) ratio alongside increased progesterone—and improved glucose metabolism and insulin sensitivity. It also normalized ovarian morphology, reduced cystic follicles, promoted follicular development, and inhibited granulosa cell apoptosis. Mechanistically, wogonin modulated the insulin signaling pathway and activated the FN1/PI3K/AKT pathway in ovarian tissues. Notably, these therapeutic effects of wogonin were substantially reversed by shFN1.
Conclusion: Wogonin exerts comprehensive therapeutic effects against IR-PCOS by targeting FN1 to activate the PI3K/AKT pathway, identifying FN1 as a key mechanistic target.

Keywords: polycystic ovary syndrome; wogonin; insulin resistance; fibronectin 1; ovarian function; PI3K/AKT

Introduction

Ovulatory dysfunction represents one of the leading causes of female infertility, imposing a significant clinical burden on reproductive health worldwide [1]. Among the various disorders leading to anovulation, polycystic ovary syndrome (PCOS) stands out as the most prevalent endocrine and metabolic disorder in women of reproductive age [2]. PCOS is clinically characterized by hyperandrogenism, chronic anovulation, and polycystic ovarian morphology, often accompanied by a luteinizing hormone (LH) to follicle-stimulating hormone (FSH) ratio imbalance [3]. Beyond its reproductive manifestations, PCOS is recognized as a multisystem condition, with frequent comorbidities including insulin resistance (IR), metabolic syndrome, non-alcoholic fatty liver disease, and an increased risk of developing type 2 diabetes, highlighting its profound long-term health implications [4].

A critical pathological link in PCOS is the coexistence of IR, which creates a self-perpetuating vicious cycle [5]. Specifically, endocrine disturbances, particularly hyperinsulinemia, exacerbate disruption of the hypothalamic-pituitary-ovarian axis, leading to aberrant androgen production and gonadotropin secretion imbalance [6]. Current management of PCOS with IR necessitates a multidisciplinary approach, incorporating lifestyle modifications, psychological interventions, and long-term pharmacotherapy [7]. However, conventional Western medicines often target single pathways, such as improving insulin sensitivity or regulating hormone levels, which may not be insufficient to address the syndrome's complexity [7].

Wogonin, a flavonoid compound extracted and isolated from the Scutellaria baicalensis Georgi (Lamiaceae) plant, exhibits a broad spectrum of pharmacological activities, including anti-inflammatory, anti-tumor, and immunomodulatory effects [8]. Recent studies have indicated its potential in improving IR [9] and its regulatory effects on multiple signaling effectors in gynecological diseases [10,11]. However, its mechanism of action in PCOS remains to be fully elucidated. We further identified wogonin and its potential target fibronectin 1 (FN1) as a core ligand-target relationship using molecular docking. Al-

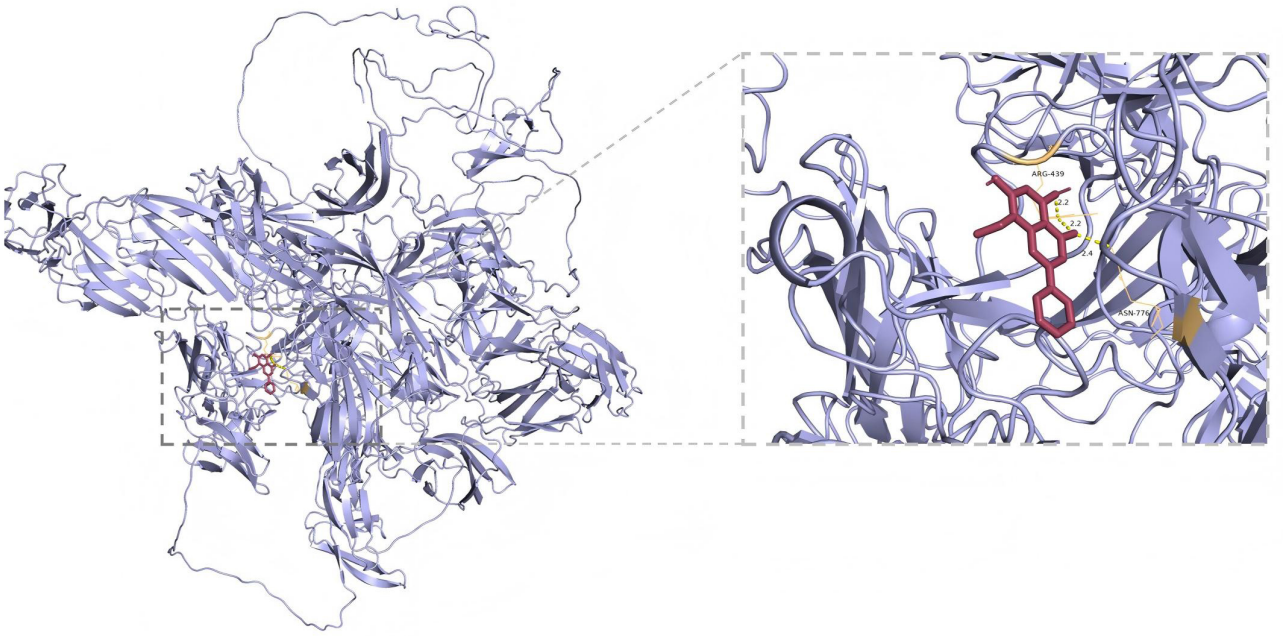

Fig. 1. Molecular docking model of wogonin and core target FN1. FN1, fibronectin 1.

though FN1 has been implicated in PCOS and is enriched in the phosphatidylinositol 3-kinase (PI3K)/Protein kinase B (AKT) signaling pathway [12], its specific role in PCOS with comorbid IR remains poorly defined. Furthermore, although the PI3K/AKT pathway is well established as a critical regulator of IR in PCOS models through regulating GLUT4-mediated glucose transport [13], the mechanistic role of the wogonin-FN1 interaction in the modulation of the FN1/PI3K/AKT axis—and its consequent effects on PCOS pathology and IR reversal—has not yet been experimentally validated.

Thus, this study aims to investigate the therapeutic effects and underlying mechanisms of wogonin using an IR-PCOS mouse model.

Materials and Methods

Molecular Docking

The protein structure of human FN1 (UniProt ID: P02751) was obtained from the AlphaFold database (model AF-P02751-F1) in PDB format, and the small molecule structure of wogonin was retrieved from the PubChem database in SDF format. Protein preparation involved removing water molecules and non-essential ligands or small molecules using PyMOL, followed by conversion of the processed structure into PDBQT format. The wogonin structure was geometrically optimized using Chem3D and subsequently converted to PDBQT format. Molecular docking was performed using AutoDock Vina to simulate and evaluate the binding interaction between wogonin and the FN1 protein.

Animal Experiments and Treatments

A total of 56 female C57BL/6J mice (6–8 weeks old, 20–25 g) at 21 days of age were obtained from the Hangzhou Medical College. The study was conducted in two sequential parts. In the first part, 24 mice were randomly assigned to three experimental groups (n = 8 per group): Control, Model, and Model + Wogonin. Control animals received standard chow and daily subcutaneous injections of sesame oil vehicle (0.1 mL per 100 g body weight). Mice in the other two groups were fed a 60% high-fat diet (HFD; Medicience Ltd., China) and administered daily subcutaneous injections of dehydroepiandrosterone (DHEA; 6 mg per 100 g body weight) for 20 consecutive days to induce a PCOS phenotype, as previously established [14]. During the subsequent 12-week treatment period, mice in the Model + Wogonin group was treated with wogonin (40 mg/kg, HY-N0400, MedChemExpress, China) via gavage, as previously described [15]. In the second part of the study, an additional 32 mice underwent the same PCOS modeling procedure (HFD + DHEA) and were then randomly divided into four groups (n = 8): Model, Model + Wogonin, Model + Wogonin + short hairpin negative control (shNC), and Model + Wogonin + shFN1. During the 12-week treatment period, mice in the Model + Wogonin, Model + Wogonin + shNC, and Model + Wogonin + shFN1 groups all received daily wogonin gavage (40 mg/kg). Additionally, mice in the Model + Wogonin + shNC and Model + Wogonin + shFN1 groups received weekly tail vein injections of shNC (target sequence: 5′-CAACAAGATGAAGAGCACCAA-3′) and shFN1 (target sequence: 5′-TGATGTCCGAACAGCTATTTA-3′,

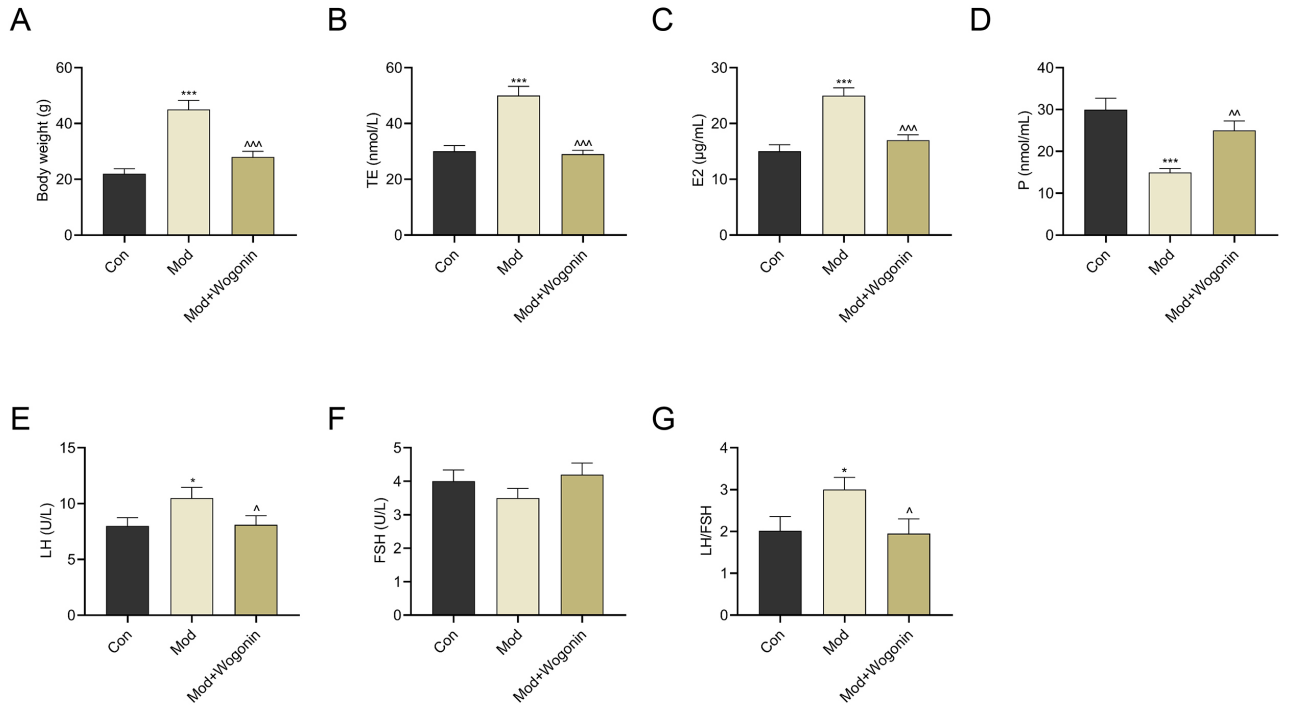

Fig. 2. Effects of wogonin on body weight and serum sex hormones in the IR-PCOS model mice. (A) Body weight of mice in different groups. (B–G) Serum levels of sex hormones in mice. (B) Testosterone (TE); (C) Estradiol (E2); (D) Progesterone (P); (E) Luteinizing hormone (LH); (F) Follicle-stimulating hormone (FSH); (G) LH/FSH ratio. Data are expressed as mean ± SD (n = 3). $*p < 0.05$, $***p < 0.001$ vs. Control; $^{\wedge}p < 0.05$, $^{\wedge\wedge}p < 0.01$, $^{\wedge\wedge\wedge}p < 0.001$ vs. Model. IR-PCOS, Insulin-resistant polycystic ovary syndrome.

shRNA_ID: Fn1_1065) lentiviral particles (VB260304-1961tte, Yunzhou Biosciences Co., Ltd., Guangzhou, China), respectively. Body weight was monitored regularly using an electronic balance. The protocol has been approved by the Institutional Animal Care and Use Committee (IACUC), Zhejiang Laboratory Animal Center (ZJCLA) (Approval No. ZJCLA-IACUC-20011081). At the end of the experiment, all mice were euthanized by cervical dislocation following deep anesthesia with 2% pentobarbital sodium (100 mg/kg, P3761, Sigma-Aldrich, St. Louis, MO, USA) via intraperitoneal injection. Death was confirmed by the absence of both heartbeat and corneal reflex for more than 5 min before the collection of serum and ovarian tissues.

Determination of Serum Sex Hormone Levels

After the last administration, mice were fasted for 8 h, and blood samples were collected from the orbital venous plexus under anesthesia induced by inhalation of 3% isoflurane (R510-22-10, RWD, Shenzhen, China). Serum was separated by centrifugation (3000 rpm, 15 min, 4 °C) and stored at –80 °C. Serum concentrations of testosterone (TE), estradiol (E2), luteinizing hormone (LH), follicle-stimulating hormone (FSH), and progesterone (P) were quantified using commercial enzyme-linked immunosorbent assay (ELISA) kits according to the manufacturer's protocols. Briefly, for T, E2, and P assays, 50 µL of sample or standard was incubated with 50 µL of HRP-conjugate for 60 min at 37 °C. For LH and FSH assays, 100 µL of sample/standard was incubated for 90 min, followed by sequential incubations with a biotinylated detection antibody for 60 min and HRP-conjugate for 30 min. After washing, all assays were incubated with substrate for 15 min, the reaction was terminated, and absorbance was immediately measured at 450 nm using a Varioskan LUX enzyme reader (Thermo Fisher, Waltham, MA, USA). Hormone concentrations were determined from standard curves, and the LH/FSH ratio was calculated based on the measured values. The specific kits employed were as follows: TE (E-OSEL-M0003), E2 (E-OSEL-M0008), LH (E-EL-M3053), FSH (E-EL-M0511), and P (E-OSEL-M0006), all from Elabscience Biotechnology Co., Ltd. (Wuhan, China).

Detection of Glucose Metabolism and IR Indicators

After the completion of the entire drug administration period, mice were fasted for 8 h, and tail vein blood glucose was measured using a blood glucose meter (Roche, Accu-Chek Active, Mannheim, Germany). Serum Fasting Insulin (FINS) levels were detected using ELISA (JL48252, JONLNBIO, Shanghai, China). The absorbance was measured using the Varioskan LUX microplate reader (Thermo Fisher Scientific, USA) at a wavelength of 450 nm. The

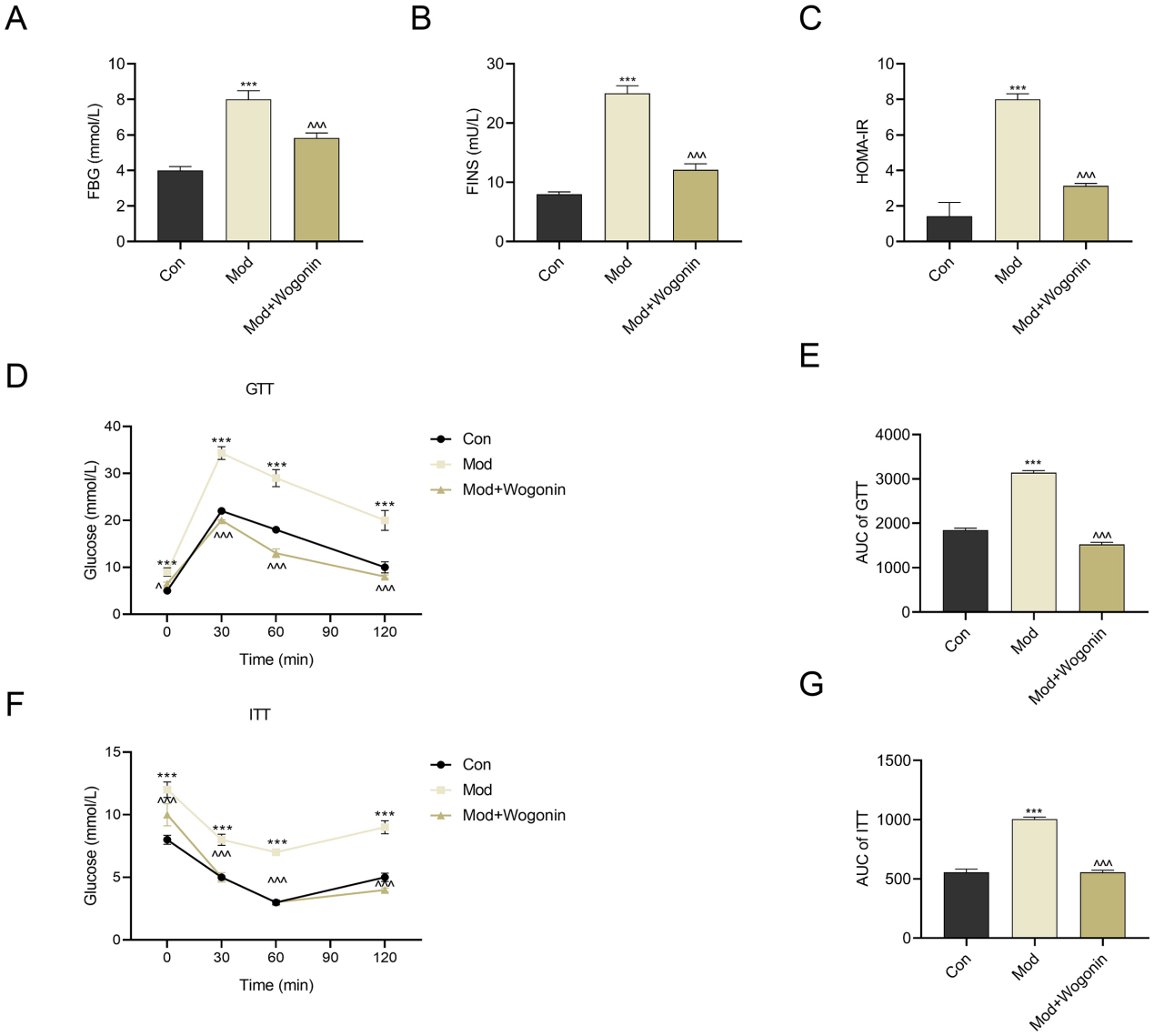

Fig. 3. Effects of wogonin on glucose metabolism and insulin resistance in the IR-PCOS model mice. (A–C) Measurement of fasting blood glucose (FBG), fasting insulin (FINS), and calculation of insulin resistance index (HOMA-IR). (D,E) Glucose tolerance test (GTT) measured using assay kit. (D) Glucose concentration curve during GTT; (E) Area under the curve of GTT (AUC of GTT). (F,G) Insulin tolerance test (ITT) measured using assay kit. (F) Glucose concentration curve during ITT; (G) Area under the curve of ITT (AUC of ITT). Data are expressed as mean ± SD (n = 3). ***$p < 0.001$ vs. Control; $^{\wedge}p < 0.05$, $^{\wedge\wedge\wedge}p < 0.001$ vs. Model.

homeostatic model assessment of IR (HOMA-IR) index was calculated using the formula: HOMA-IR = fasting blood glucose (FBG) (mmol/L) × FINS (mIU/L) / 22.5.

Glucose Tolerance Test (GTT)

After the completion of the entire drug administration period, mice were fasted for 12 h, then intraperitoneally injected with D-glucose (2 g/kg body weight). Tail vein blood glucose was measured at 0, 30, 60, and 120 min after injection using the same portable blood glucose meter (Roche, Accu-Chek Active, Mannheim, Germany). The area under the glucose curve ($AUC_{0–120}$) was calculated using the trapezoidal method to evaluate glucose tolerance.

Insulin Tolerance Test (ITT)

After the completion of the entire drug administration period, mice were fasted for 4 h, then intraperitoneally injected with insulin (0.75 U/kg body weight). Tail vein blood glucose was measured at 0, 30, 60, and 120 min after injection using the same portable blood glucose meter (Roche, Accu-Chek Active, Mannheim, Germany). The $AUC_{0–120}$ was calculated to assess insulin sensitivity.

Organ Index Measurement

After blood collection, mice were euthanized by cervical dislocation. Ovaries, uterus, and perirenal were dis-

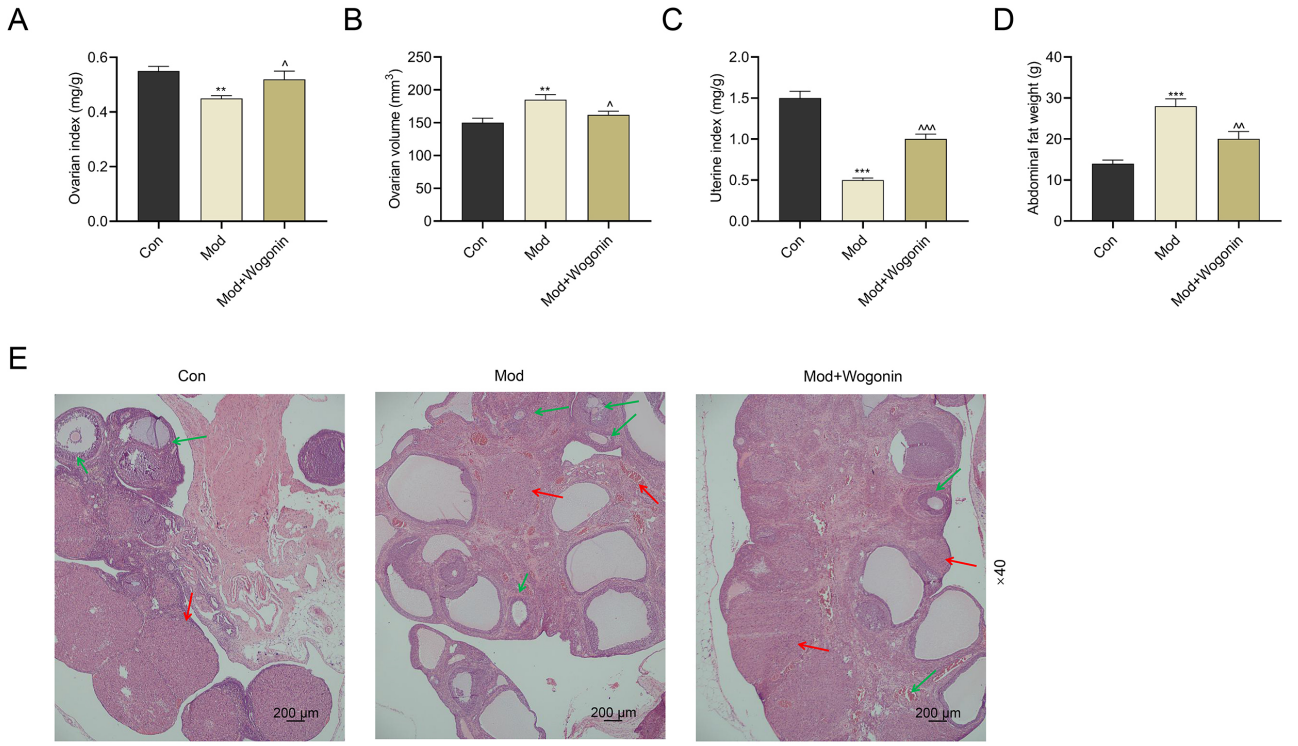

Fig. 4. Effects of wogonin on organ indices and ovarian histomorphology in the IR-PCOS model mice. (A–D) Calculation of organ indices. (A) Ovarian index (ovarian weight/body weight, mg/g); (B) Ovarian volume (mm^3); (C) Uterine index (uterine weight/body weight, mg/g); (D) Abnormal fat weight (g). (E) Histomorphological changes of ovarian tissues detected using H&E staining (×40 magnification, scale bar = 200 μm). Red arrows indicate the corpus luteum, and the green arrows indicate the follicle. Data are expressed as mean ± SD (n = 3). $^{**}p < 0.01$, $^{***}p < 0.001$ vs. Control; $^{\wedge}p < 0.05$, $^{\wedge\wedge}p < 0.01$, $^{\wedge\wedge\wedge}p < 0.001$ vs. Model.

sected, rinsed with normal saline, and blotted dry to remove surface moisture. The wet weight of each organ was measured using an electronic balance. The ovarian/uterine index was calculated as: ovarian/uterine index (mg/g) = ovarian/uterine wet weight (mg) / mouse body weight (g). Ovarian volume was measured using a vernier caliper (long diameter × short diameter ^{2} × π/6).

Hematoxylin and Eosin (H&E) Staining

Ovarian tissues were harvested and fixed in 4% paraformaldehyde (TW26423, TW-reagent, Nanjing, China) for 24 hours at 4 °C. Following fixation, the samples were subjected to routine paraffin embedding and sectioned at a thickness of 4 μm. The sections were subsequently dewaxed in xylene and rehydrated through a graded ethanol series. Staining was performed using a commercial H&E kit (GF11014, Glpbio, Montclair, CA, USA), following the manufacturer's instructions. Briefly, sections were deparaffinized using xylene, rehydrated by gradient ethanol, and stained with hematoxylin (HY-N0116, MedChemExpress, Monmouth Junction, NJ, USA) for 8 min. The stained sections were differentiated using 1% hydrochloric alcohol, and treated with weakly alkaline water (67362, Sigma-Aldrich, St. Louis, MO, USA) to develop blue coloration. Sections were then counterstained with eosin (HY-D0505A, MedChemExpress, Monmouth Junction, NJ, USA) for 5 min, followed by dehydration, clearing, and mounting with coverslips. Histological examination was performed under a light microscope (KD-810A, KDYXBIO, Nanjing, China), and images were captured for subsequent analysis.

Terminal Deoxynucleotidyl Transferase dUTP Nick End Labeling (TUNEL)

Apoptosis in ovarian granulosa cells was assessed by the TUNEL assay using a commercial detection kit (C1086, Beyotime, Shanghai, China). Briefly, paraffin-embedded sections were first deparaffinized and rehydrated. The tissues were then digested with Proteinase K (ST532, Beyotime, Shanghai, China) at 37 °C for 20 min to achieve antigen retrieval. Subsequently, the sections were incubated with the TUNEL reaction mixture for 60 min at 37 °C in a humidified dark chamber. Cell nuclei were counterstained with DAPI (T19827, TargetMol, Boston, MA, USA) for 5 min. Fluorescent images were finally acquired using an Olympus IX73 microscope at 200× magnification.

Western Blotting

Protein samples from the ovarian tissues were extracted with radio-immunoprecipitation assay (RIPA) Lysis

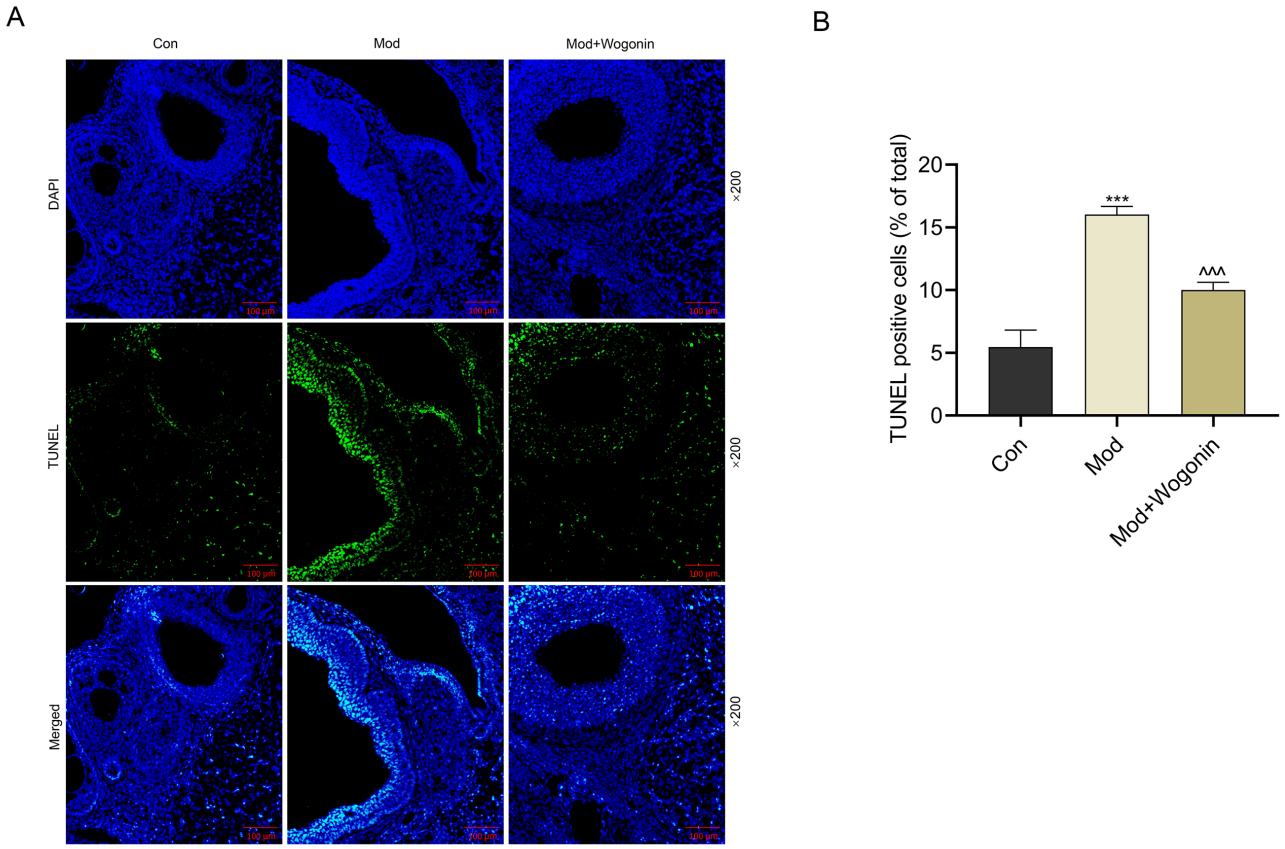

Fig. 5. Detection of ovarian granulosa cell apoptosis by TUNEL staining. (A,B) TUNEL staining was performed to assess apoptosis of ovarian granulosa cells. DAPI (blue) stains cell nuclei, TUNEL (green) labels apoptotic cells, and the "Merged" panel is the combined image. Images were captured at ×200 magnification, with a scale bar of 100 µm. Data are expressed as mean ± SD (n = 3). ***$p < 0.001$ vs. Control; $^{\wedge\wedge\wedge}p < 0.001$ vs. Model. TUNEL, Terminal deoxynucleotidyl transferase dUTP nick end labeling; DAPI, 4′,6-diamidino-2-phenylindole.

Buffer (AP01L013, Life-iLab, Shanghai, China) and quantified using a bicinchoninic acid (BCA) assay (YWB002, YFXBIO, Shanghai, China). Following separation via sodium dodecyl sulfate–polyacrylamide gel electrophoresis (SDS-PAGE) (190916-40, YaJi Biological, Shanghai, China), the proteins were transferred onto polyvinylidene fluoride (PVDF) membranes (WJ001S, epizyme, Shanghai, China). After blocking with a specialized buffer (AP36L118, Life-iLab, Shanghai, China) to prevent non-specific binding, the membranes were probed with primary antibodies (Table 1) at 4 °C overnight. After washing, the membranes were incubated with HRP-linked secondary antibodies (Table 1). The antigen-antibody complexes were detected using enhanced chemiluminescence (ECL kit YWB003, YFXBIO, Shanghai, China), and the signals were documented with a SynGene imaging system (G:BOX F3, Syngene, Cambridge, UK). Protein expression levels were normalized to the endogenous control glyceraldehyde 3-phosphate dehydrogenase (GAPDH). Data are expressed as fold change relative to the control (con) group.

Statistical Analysis

All experiments were performed in at least three independent replicates. One-way analysis of variance (ANOVA) followed by Tukey's post hoc test was used for comparison among groups, while repeated measures ANOVA followed by Tukey's post hoc test was applied for comparisons across different time points. Data were analyzed using SPSS 21.0 system (SPSS Inc., Chicago, IL, USA) and are expressed as the Mean ± standard deviation. A $p < 0.05$ was considered statistically significant.

Results

Wogonin Regulates Body Weight and Serum Sex Hormones in IR-PCOS Mice

Molecular docking analysis showed that wogonin formed a stable binding with FN1, establishing 3 hydrogen bonds and exhibiting a binding free energy of –7.5 kcal/mol (Fig. 1).

In the IR-PCOS model mice, body weight was significantly increased, while wogonin treatment reduced body

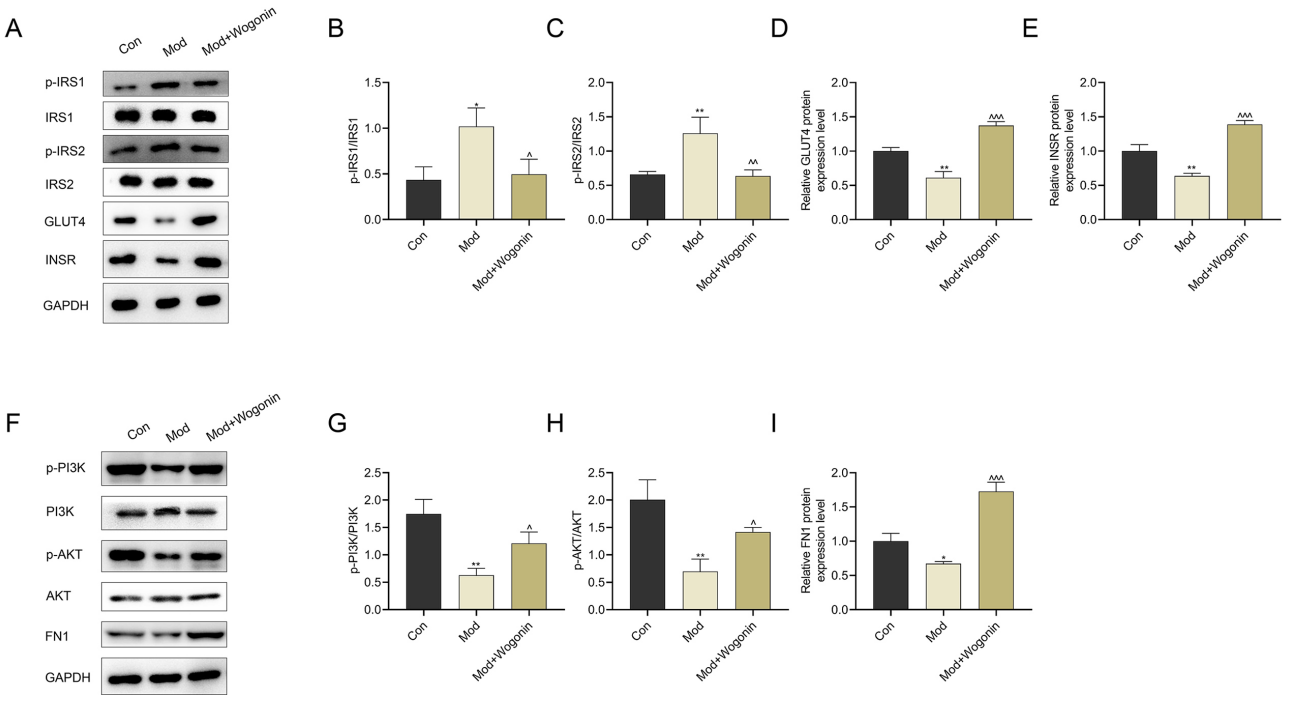

Fig. 6. Effects of wogonin on the insulin signaling pathway and FN1/PI3K/AKT pathway proteins in ovarian tissues. (A–E) Western blot detection of the insulin signaling pathway proteins in ovarian tissues. (F–I) Western blot detection of the FN1/PI3K/AKT pathway proteins in ovarian tissues. Data are expressed as mean ± SD (n = 3). *$p < 0.05$, **$p < 0.01$ vs. Control; ^$p < 0.05$, ^^$p < 0.01$, ^^^$p < 0.001$ vs. Model.

Table 1. Antibodies used in this study.

Name	Catalog	Dilution	Manufacturer
p-IRS1	AF3272	1/1000	Affinity, USA
IRS1	AF6273	1/1000	Affinity, USA
p-IRS2	PA5-106094	1/1000	ThermoFisher, USA
IRS2	DF7534	1/1000	Affinity, USA
GLUT4	AF5386	1/1000	Affinity, USA
INSR	AF6099	1/1000	Affinity, USA
p-PI3K	AF3242	1/1000	Affinity, USA
PI3K	ab140307	1/1000	abcam, UK
p-AKT	AF0016	1/1000	Affinity, USA
AKT	AF6261	1/1000	Affinity, USA
FN1	ab2413	1/1000	abcam, UK
GAPDH	ab8245	1/10,000	abcam, UK
Goat anti-rabbit	ab205718	1/2000	abcam, UK
Goat anti-mouse	ab205719	1/2000	abcam, UK

Abbreviations: p-IRS1, phosphorylated insulin receptor substrate 1; IRS1, insulin receptor substrate 1; p-IRS2, phosphorylated insulin receptor substrate 2; IRS2, insulin receptor substrate 2; GLUT4, glucose transporter type 4; INSR, insulin receptor; p-PI3K, phosphorylated phosphatidylinositol 3-kinase; PI3K, phosphatidylinositol 3-kinase; p-AKT: phosphorylated protein kinase B; AKT, protein kinase B; FN1, fibronectin 1; GAPDH, glyceraldehyde-3-phosphate dehydrogenase.

weight (Fig. 2A, $p < 0.05$). For serum sex hormones, TE, E2, LH, and the LH/FSH ratio were significantly elevated in the Model group (Fig. 2B,C,E,G, $p < 0.05$), whereas P was significantly decreased (Fig. 2D, $p < 0.05$). FSH showed no significant difference among all groups (Fig. 2F). Notably, wogonin treatment significantly decreased TE, E2, LH, and the LH/FSH ratio, and increased P (Fig. 2B–E,G, $p < 0.05$).

Wogonin Improves Glucose Metabolism and IR in IR-PCOS Mice

IR-PCOS model mice showed elevated FBG, FINS, and the HOMA-IR index, indicating the presence of IR (Fig. 3A–C, $p < 0.05$). Wogonin treatment improved these indicators (Fig. 3A–C, $p < 0.05$). The GTT and ITT showed that glucose metabolism and insulin sensitivity were enhanced by wogonin (Fig. 3D–G, $p < 0.05$).

Wogonin Improves Ovarian Histomorphology, Organ Indices, and Inhibits Granulosa Cell Apoptosis in IR-PCOS Mice

Evaluation of organometric parameters revealed profound disruptions in both metabolic and reproductive physiology in the IR-PCOS model mice. Specifically, significant elevation in ovarian volume and abnormal fat mass were observed, accompanied by a pronounced reduction in the ovarian index and uterine index relative to control animals (Fig. 4A–D, $p < 0.05$). Administration of wogonin effec-

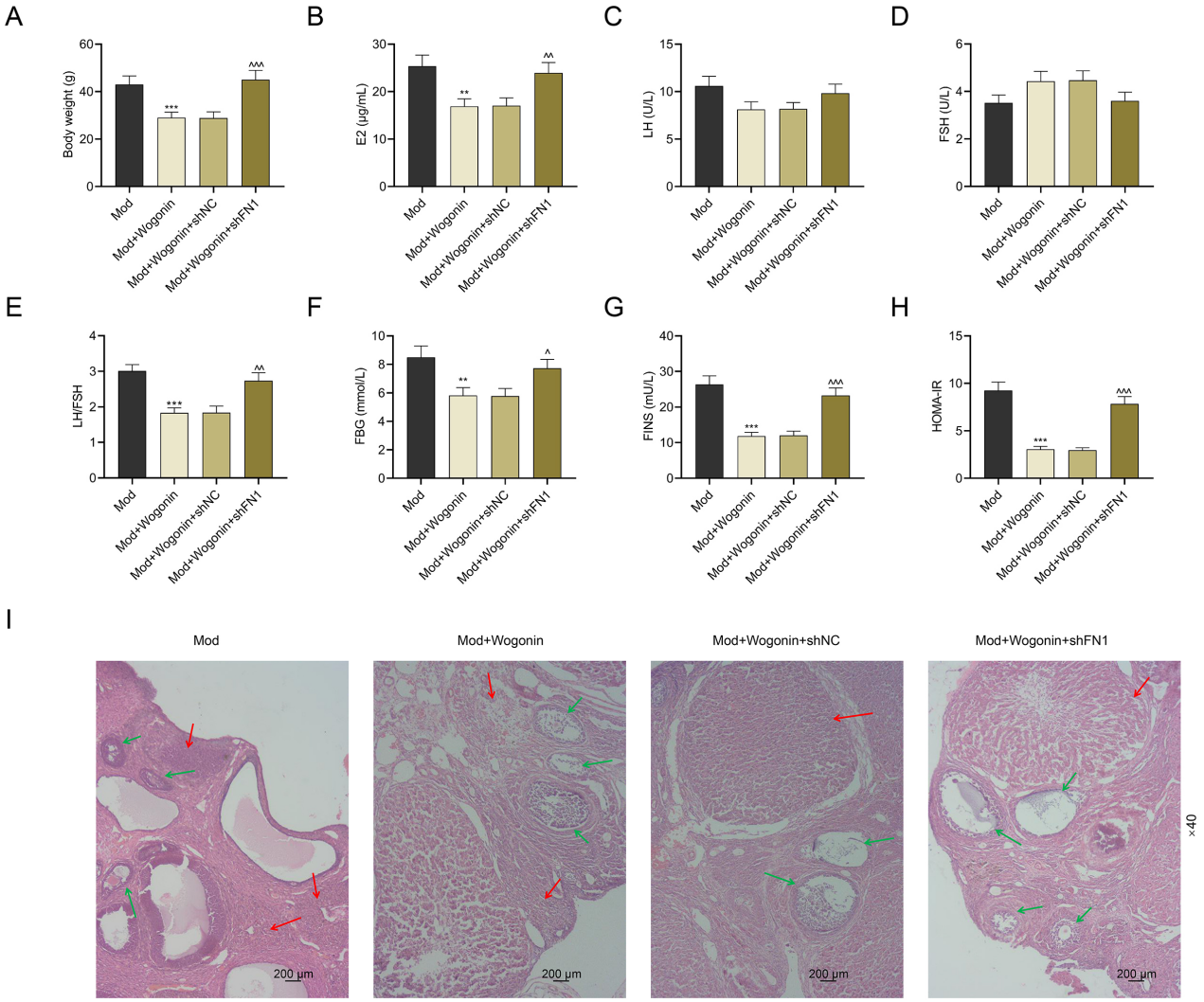

Fig. 7. Wogonin regulates the body weight, serum sex hormones and ovarian histomorphology in the IR-PCOS model mice through FN1. (A) Body weight of mice in different groups. (B–E) Serum levels of sex hormones in mice. (B) Estradiol (E2); (C) Luteinizing hormone (LH); (D) Follicle-stimulating hormone (FSH); (E) LH/FSH ratio. (F–H) Measurement of FBG, FINS, and calculation of insulin resistance index (HOMA-IR). (I) Histomorphological changes of ovarian tissues detected using H&E staining (×40 magnification, scale bar = 200 μm). Red arrows indicate the corpus luteum, and the green arrows indicate the follicle. Data are expressed as mean ± SD (n = 3). $^{**}p < 0.01$, $^{***}p < 0.001$ vs. Mod; $^{\wedge}p < 0.05$, $^{\wedge\wedge}p < 0.01$, $^{\wedge\wedge\wedge}p < 0.001$ vs. Mod + Wogonin + shNC.

tively counteracted these pathological alterations, restoring all measured parameters toward normal levels (Fig. 4A–D, $p < 0.05$).

Histopathological examination via H&E staining further corroborated the ovarian dysfunction. Control ovaries displayed normal folliculogenesis, featuring multiple corpora lutea and antral follicles with up to 8–9 layers of granulosa cells. In contrast, ovarian sections from the Model group exhibited significant morphological disruption, predominantly manifested as cystic follicular dilatation with absent oocytes and disrupted corona radiata. Therapeutic intervention with wogonin ameliorated ovarian architecture, as characterized by the observation of follicles at various developmental stages, increased corpora lutea formation, and reduced cystic follicles (Fig. 4E). Additionally, TUNEL staining showed that the apoptosis of ovarian granulosa cells was increased in the IR-PCOS model mice, while wogonin treatment reduced the apoptotic rate, as indicated by decreased TUNEL-positive cells (Fig. 5).

Wogonin Regulates Insulin Signaling Pathway and FN1/PI3K/AKT Pathway in Ovarian Tissues of IR-PCOS Mice

Western blot analysis revealed that in ovarian tissues of IR-PCOS model mice, the levels of p-IRS1/IRS1 and p-IRS2/IRS2 were significantly elevated, while the expression levels of GLUT4 and INSR were decreased (Fig. 6A–E, $p < 0.05$). Additionally, in the FN1/PI3K/AKT pathway,

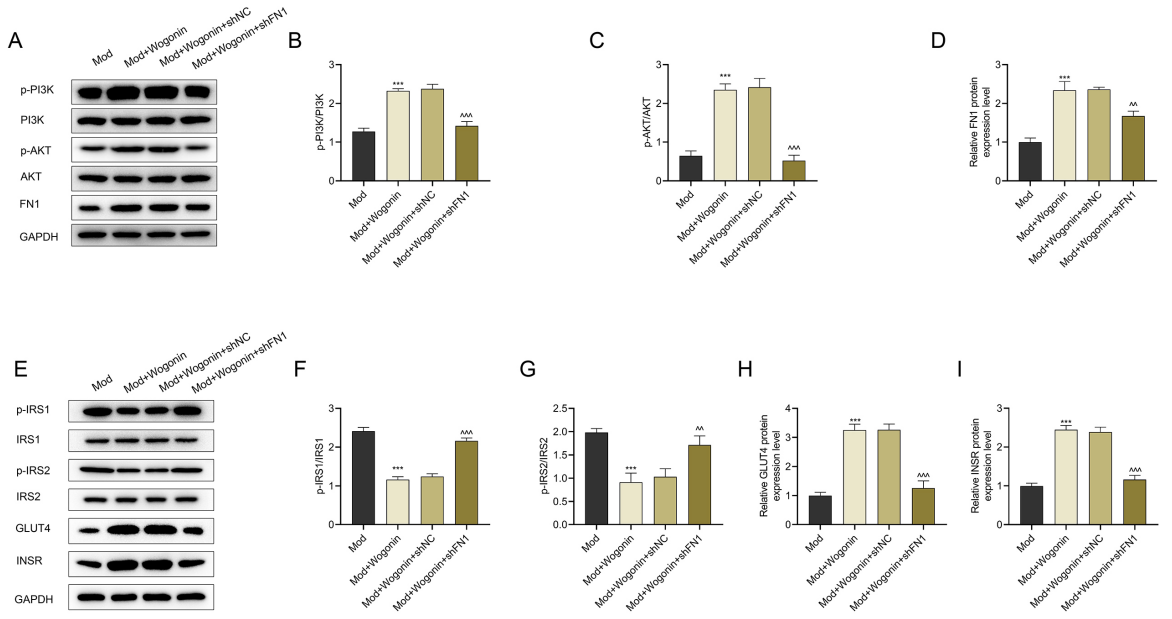

Fig. 8. Wogonin regulates the insulin signaling pathway and FN1/PI3K/AKT pathway proteins in ovarian tissues through FN1. (A–D) Western blot detection of the FN1/PI3K/AKT pathway proteins in ovarian tissues. (E–I) Western blot detection of the insulin signaling pathway proteins in ovarian tissues. Data are expressed as mean ± SD (n = 3). ***$p < 0.001$ vs. Mod; ^^$p < 0.01$, ^^^$p < 0.001$ vs. Mod + Wogonin + shNC.

the levels of p-PI3K/PI3K, p-AKT/AKT, and the expression level of FN1 were notably reduced in the Model group (Fig. 6F–I, $p < 0.05$). Importantly, wogonin treatment reversed these abnormal changes, thereby modulating the insulin signaling pathway and activating the FN1/PI3K/AKT pathway (Fig. 6A–I, $p < 0.05$).

Wogonin Ameliorates Multiple Pathological Phenotypes of IR-PCOS Mice via FN1

To explore the regulatory effects of wogonin and FN1 on IR-PCOS, female C57BL/6J mice were established as IR-PCOS models, then treated with wogonin plus shFN1 or shNC. Wogonin reduced the body weight of model mice, while FN1 silencing reversed this effect (Fig. 7A, $p < 0.05$). For serum sex hormones, wogonin alleviated the increased E2 levels and LH/FSH ratio in Mod mice, which was also abrogated by shFN1 (Fig. 7B–E, $p < 0.05$). Regarding insulin resistance, wogonin lowered the FBG, FINS, and HOMA-IR in Mod mice, with this improvement reversed by FN1 silencing (Fig. 7F–H, $p < 0.05$). Histologically, wogonin ameliorated the follicular cystic dilatation in Mod mouse ovaries, while shFN1 aggravated this lesion again (Fig. 7I). At the molecular level, wogonin normalized the abnormal PI3K/AKT pathway and insulin signaling pathway proteins in ovarian tissues (upregulated p-PI3K/PI3K, p-AKT/AKT, FN1, GLUT4 and INSR, and reduced p-IRS1/IRS1 and p-IRS2/IRS2 ratios) in Mod mice, and these regulatory effects were reversed by FN1 silencing (Fig. 8A–I, $p < 0.05$).

Discussion

This investigation provides a systematic delineation of the therapeutic mechanisms of wogonin in a murine model of IR-PCOS. The central finding was the identification of the FN1/PI3K/AKT signaling axis as a concrete pathway.

Administration of wogonin markedly alleviated the core pathological features in the IR-PCOS model. Metabolically, treatment led to significant reductions in body weight, fasting glucose, and insulin levels, concomitant with enhanced insulin sensitivity. These outcomes are consistent with previously documented metabolic benefits of wogonin [9]. Endocrinological profiling revealed a reversal of the characteristic steroidogenic disturbances in PCOS, evidenced by decreased testosterone, estradiol, and the LH/FSH ratio, along with elevated progesterone. In this study, the ability of wogonin to normalize sex hormone levels represents a novel finding. Morphologically, ovarian histology demonstrated that wogonin reduced cystic follicle prevalence, supported the orderly development of follicles and corpus luteum formation, and significantly attenuated granulosa cell apoptosis. These results underscore the context-dependent nature of wogonin, which exerts pro-apoptotic actions in malignancies [16,17] but demonstrates cytoprotective effects in normal cellular environments [18,19].

A pivotal finding of this work is the mechanistic link to the FN1/PI3K/AKT pathway. We found that wogonin restored the phosphorylation status of IRS1 and IRS2 in ovar-

ian tissue, while upregulating the expression of INSR and the glucose transporter GLUT4. This indicates a comprehensive amelioration of IR, encompassing not only peripheral tissues but, crucially, the restoration of defective insulin signaling within the ovary itself [20,21]. Furthermore, we identified FN1, an extracellular matrix glycoprotein, as a potential upstream mediator. Supported by molecular docking analyses indicating a stable interaction between wogonin and FN1, our *in vivo* experiments confirmed a significant downregulation of FN1 in PCOS ovaries, which was effectively rescued by treatment. Given that FN1 is a known activator of the PI3K/AKT cascade via integrin binding [22], the subsequent recovery of PI3K and AKT phosphorylation observed in our study delineates a plausible signaling sequence. The activation of AKT, a central hub in this pathway, underlies key therapeutic outcomes: it facilitates GLUT4 membrane translocation, thereby augmenting insulin sensitivity [23], and concurrently exerts potent anti-apoptotic effects [24], providing a molecular rationale for the suppressed granulosa cell apoptosis detected in TUNEL assays. These findings align with documented roles of wogonin in modulating AKT/GLUT4 signaling in metabolic contexts [25]. Although PI3K/AKT dysregulation has been implicated in PCOS pathogenesis [26–28], the novel aspect of our study lies in connecting the therapeutic effects of wogonin to the upregulation of FN1, thereby initiating a protective signaling cascade that concurrently tackles IR and cellular apoptosis in the ovary.

This study has several limitations. Although the animal model recapitulates the major features of the human condition, it cannot fully reflect the etiological complexity of PCOS.

Conclusion

In conclusion, this study is the first to systematically demonstrate the comprehensive therapeutic effects of wogonin on metabolic, hormonal, ovarian morphological, and apoptotic aspects in an IR-PCOS mouse model. These findings highlight the considerable potential of wogonin, a natural product, as a multi-target, integrated therapeutic agent for PCOS.

Availability of Data and Materials

The datasets used or analyzed during the current study are available from the corresponding author upon reasonable request.

Author Contributions

LY and FZ designed the research study; LY, FZ, DL and MZ performed the research; LY, DL and WS collected and analyzed the data. LY, FZ and WS have been involved in drafting the manuscript and all authors have been involved in revising it critically for important intellectual content. All authors gave final approval of the version to be published. All authors have participated sufficiently in the work to take public responsibility for appropriate portions of the content and agreed to be accountable for all aspects of the work in ensuring that questions related to its accuracy or integrity.

Ethics Approval and Consent to Participate

All animal experiments have been approved by the Institutional Animal Care and Use Committee (IACUC), Zhejiang Laboratory Animal Center (ZJCLA) (Approval No. ZJCLA-IACUC-20011081).

Acknowledgment

Not applicable.

Funding

This work was supported by the Traditional Chinese Medicine Science and Technology Program of Zhejiang Province [grant number: 2024ZL136] and the Medical and Health Science and Technology Project of Hangzhou City [grant number: B20241610].

Conflict of Interest

The authors declare no conflict of interest.

References

[1] Carson SA, Kallen AN. Diagnosis and Management of Infertility: A Review. JAMA. 2021; 326: 65–76. https://doi.org/10.1001/jama.2021.4788.

[2] Stener-Victorin E, Teede H, Norman RJ, Legro R, Goodarzi MO, Dokras A, *et al*. Polycystic ovary syndrome. Nature Reviews. Disease Primers. 2024; 10: 27. https://doi.org/10.1038/s41572-024-00511-3.

[3] Yang J, Chen C. Hormonal changes in PCOS. The Journal of Endocrinology. 2024; 261: e230342. https://doi.org/10.1530/JOE-23-0342.

[4] Kim KW. Unravelling Polycystic Ovary Syndrome and Its Comorbidities. Journal of Obesity & Metabolic Syndrome. 2021; 30: 209–221. https://doi.org/10.7570/jomes21043.

[5] Zhao H, Zhang J, Cheng X, Nie X, He B. Insulin resistance in polycystic ovary syndrome across various tissues: an updated review of pathogenesis, evaluation, and treatment. Journal of Ovarian Research. 2023; 16: 9. https://doi.org/10.1186/s13048-022-01091-0.

[6] Armanini D, Boscaro M, Bordin L, Sabbadin C. Controversies in the Pathogenesis, Diagnosis and Treatment of PCOS: Focus on Insulin Resistance, Inflammation, and Hyperandrogenism. International Journal of Molecular Sciences. 2022; 23: 4110. https://doi.org/10.3390/ijms23084110.

[7] Hoeger KM, Dokras A, Piltonen T. Update on PCOS: Consequences, Challenges, and Guiding Treatment. The Journal of Clinical Endocrinology and Metabolism. 2021; 106: e1071–e1083. https://doi.org/10.1210/clinem/dgaa839.

[8] Huynh DL, Ngau TH, Nguyen NH, Tran GB, Nguyen CT. Potential therapeutic and pharmacological effects of Wogonin: an

updated review. Molecular Biology Reports. 2020; 47: 9779–9789. https://doi.org/10.1007/s11033-020-05972-9.

[9] Zhou Z, Wang M, Zhang X, Xu Y, Li P, Zheng Z, *et al*. Synergistic potential of Berberine and Wogonin improved adipose inflammation and insulin resistance associated with obesity through HIF-α axis. Chinese Medicine. 2025; 20: 155. https://doi.org/10.1186/s13020-025-01223-w.

[10] Meresman GF, Götte M, Laschke MW. Plants as source of new therapies for endometriosis: a review of preclinical and clinical studies. Human Reproduction Update. 2021; 27: 367–392. https://doi.org/10.1093/humupd/dmaa039.

[11] Fang DN, Zheng CW, Ma YL. Effectiveness of Scutellaria baicalensis Georgi root in pregnancy-related diseases: A review. Journal of Integrative Medicine. 2023; 21: 17–25. https://doi.org/10.1016/j.joim.2022.09.005.

[12] Zhou F, Xing Y, Cheng T, Yang L, Ma H. Exploration of hub genes involved in PCOS using biological informatics methods. Medicine. 2022; 101: e30905. https://doi.org/10.1097/MD.0000000000030905.

[13] Zhang N, Liu X, Zhuang L, Liu X, Zhao H, Shan Y, *et al*. Berberine decreases insulin resistance in a PCOS rats by improving GLUT4: Dual regulation of the PI3K/AKT and MAPK pathways. Regulatory Toxicology and Pharmacology. 2020; 110: 104544. https://doi.org/10.1016/j.yrtph.2019.104544.

[14] Wu H, Zhao B, Yao Q, Kang J. Dehydroepiandrosterone-induced polycystic ovary syndrome mouse model requires continous treatments to maintain reproductive phenotypes. Journal of Ovarian Research. 2023; 16: 207. https://doi.org/10.1186/s13048-023-01299-8.

[15] Liu Y, Zhang M, Zeng L, Lai Y, Wu S, Su X. Wogonin upregulates SOCS3 to alleviate the injury in Diabetic Nephropathy by inhibiting TLR4-mediated JAK/STAT/AIM2 signaling pathway. Molecular Medicine. 2024; 30: 78. https://doi.org/10.1186/s10020-024-00845-4.

[16] Lin Y, Jiang X, Zhao M, Li Y, Jin L, Xiang S, *et al*. Wogonin induces mitochondrial apoptosis and synergizes with venetoclax in diffuse large B-cell lymphoma. Toxicology and Applied Pharmacology. 2024; 492: 117103. https://doi.org/10.1016/j.taap.2024.117103.

[17] Wu K, Teng M, Zhou W, Lu F, Zhou Y, Zeng J, *et al*. Wogonin Induces Cell Cycle Arrest and Apoptosis of Hepatocellular Carcinoma Cells by Activating Hippo Signaling. Anti-Cancer Agents in Medicinal Chemistry. 2022; 22: 1551–1560. https://doi.org/10.2174/1871520621666210824105915.

[18] Wei Y, Zhao J, Xiong J, Chai J, Yang X, Wang J, *et al*. Wogonin reduces cardiomyocyte apoptosis from mitochondrial release of cytochrome *c* to improve doxorubicin-induced cardiotoxicity. Experimental and Therapeutic Medicine. 2022; 23: 205. https://doi.org/10.3892/etm.2022.11128.

[19] Feng Y, Ju Y, Yan Z, Ji M, Yang M, Wu Q, *et al*. Protective role of wogonin following traumatic brain injury by reducing oxidative stress and apoptosis via the PI3K/Nrf2/HO 1 pathway. International Journal of Molecular Medicine. 2022; 49: 53. https://doi.org/10.3892/ijmm.2022.5109.

[20] Copps KD, White MF. Regulation of insulin sensitivity by serine/threonine phosphorylation of insulin receptor substrate proteins IRS1 and IRS2. Diabetologia. 2012; 55: 2565–2582. https://doi.org/10.1007/s00125-012-2644-8.

[21] Pervaz S, Ullah A, Adu-Gyamfi EA, Lamptey J, Sah SK, Wang MJ, *et al*. Role of CPXM1 in Impaired Glucose Metabolism and Ovarian Dysfunction in Polycystic Ovary Syndrome. Reproductive Sciences. 2023; 30: 526–543. https://doi.org/10.1007/s43032-022-00987-y.

[22] Mao XG, Xue XY, Lv R, Ji A, Shi TY, Chen XY, *et al*. CEBPD is a master transcriptional factor for hypoxia regulated proteins in glioblastoma and augments hypoxia induced invasion through extracellular matrix-integrin mediated EGFR/PI3K pathway. Cell Death & Disease. 2023; 14: 269. https://doi.org/10.1038/s41419-023-05788-y.

[23] Luo W, Ai L, Wang BF, Zhou Y. High glucose inhibits myogenesis and induces insulin resistance by down-regulating AKT signaling. Biomedicine & Pharmacotherapy. 2019; 120: 109498. https://doi.org/10.1016/j.biopha.2019.109498.

[24] Gao Y, Chen J, Ji R, Ding J, Zhang Y, Yang J. USP25 Regulates the Proliferation and Apoptosis of Ovarian Granulosa Cells in Polycystic Ovary Syndrome by Modulating the PI3K/AKT Pathway *via* Deubiquitinating PTEN. Frontiers in Cell and Developmental Biology. 2021; 9: 779718. https://doi.org/10.3389/fcell.2021.779718.

[25] Khan S, Kamal MA. Wogonin Alleviates Hyperglycemia Through Increased Glucose Entry into Cells Via AKT/GLUT4 Pathway. Current Pharmaceutical Design. 2019; 25: 2602–2606. https://doi.org/10.2174/1381612825666190722115410.

[26] Wang K, Li Y. Signaling pathways and targeted therapeutic strategies for polycystic ovary syndrome. Frontiers in Endocrinology. 2023; 14: 1191759. https://doi.org/10.3389/fendo.2023.1191759.

[27] Ma Y, Ma Y, Li P, Ma F, Yu M, Xu J, *et al*. Wnt5a alleviates the symptoms of PCOS by modulating PI3K/AKT/mTOR pathway-mediated autophagy in granulosa cells. Cellular Signalling. 2025; 127: 111575. https://doi.org/10.1016/j.cellsig.2024.111575.

[28] Lin W, Wang Y, Zheng L. Polycystic ovarian syndrome (PCOS) and recurrent spontaneous abortion (RSA) are associated with the PI3K-AKT pathway activation. PeerJ. 2024; 12: e17950. https://doi.org/10.7717/peerj.17950.